TEL AVIV UNIVERSITY
RAYMOND AND BEVERLY SACKLER
FACULTY OF EXACT SCIENCES
BLAVATNIK SCHOOL OF COMPUTER SCIENCE

Computer Analysis of the Dead Sea Scroll Manuscripts

Thesis submitted in partial fulfillment of the requirements for the M.Sc. degree in the School of Computer Science, Tel Aviv University

by

Tamar Lavee

The research for this thesis has been carried out at Tel Aviv University under the supervision of Prof. Nachum Dershowitz

September 2013

Abstract

The Dead Sea Scrolls were discovered in the Qumran area and elsewhere in the Judean desert beginning in 1947 and were photographed in infrared during the 1950s. Recently, the Israel Antiquities Authority embarked on an ambitious project to digitize all the fragments using multi-spectral cameras and make them available on-line.

The use of computerized tools to investigate images of historical documents has been shown to produce significant contributions in the historical study of the Cairo Genizah and many other collections. Such tools may contribute to the resolution of open questions related to research on the scrolls, such as who wrote the scrolls, and to facilitate piecing together the fragments of the scrolls.

This work deals with initial steps of image processing of the scrolls, focusing on two main problems: image binarization and character recognition. We developed two methods of obtaining high quality binary images of the scrolls. The first method is based on the multi-spectral images taken at different wavelengths. We show that the use of different wavelength of the same image allows us to produce a more informative binary image. The second method combines the results of several binarization methods to build an accurate classifier that separates between the text and the background of the fragments.

Finally, we adapt a keypoint detection method based on the identification of connected components in the image, to locate the letters in the images. We use a character spotting technique to search for a given query letter within these keypoints. This technique extracts features from the image that are shown to differentiate between Hebrew characters, and uses a Dynamic Time Warping algorithm to compare different features of letters. We show that this approach is capable of distinguishing between different scripts of the scrolls, and thus, it may by used to identify fragments written by the same hand.

Contents

Chapter 1

Introduction

The Dead Sea Scrolls were written between the third century BCE and the first CE, and were discovered in the Qumran area and elsewhere in the Judean desert beginning in 1947. These fragmentary documents have taught the world a great deal about Jewish history in the late Second Temple period and about sectarian Judaism, and they have provided much background knowledge relevant to the birth of Christianity. In addition, the Dead Sea Scrolls have enhanced our understanding of the textual transmission of the Bible. Following their discovery, all the scrolls were photographed using infrared (IR) film and Kodak filters [1].

The Israel Antiquities Authority, in collaboration with Google, Inc., has recently embarked on an ambitious project to digitize all the fragments using multi-spectral cameras and make the images available on the Internet [2]. As a result, scholars will soon be faced with thousands of fragmentary documents, but without computer aids that would make it possible to find sought-after needles in a proverbial haystack of on-line images. The problems are even more acute since optical character recognition does not provide quality searchable texts for such historical documents.

This work deals with initial steps of image processing of the scrolls, focusing on two main problems: image binarization and character recognition. These are essential steps in many possible applications and techniques that will enable further exploration of these images, such as OCR, palaeographic classification, joins identification and more.

Image binarization is the process of separating the foreground, namely, the text, from the background, providing a black-and-white binary image. This is an essential stage of every document image-processing system. In images of historical manuscripts such as the scrolls this is a very challenging task, as degradation and different kinds of damage lead to variability both in the background and in the foreground. Many methods have been suggested to binarize non-uniform document images ([3, 4]). Other methods have been proposed to solve typical problems of historical documents ([5, 6]). In this work we investigate the results of known binarization methods on the Dead Sea scrolls, and we propose different methods of combinations between the different algorithms. Another suggested approach is to use the information captured in images taken in different wavelength, as are available for the scrolls.

After obtaining a binary image, the next step is to identify the characters in the image. In [7], a method has been suggested to detect Hebrew letters in the Cairo Genizah, based on the fact that in Hebrew script, the letters are not connected. We apply this method and adapt it to the images of the scrolls, and use the obtained information in order to improve the binarization result. We use the achieved keypoints as candidates for a character spotting algorithm, aiming to identify the correct letter in the keypoint, and to distinguish between the different scripts of the fragments.

The structure of the thesis is as follows. In Chapter 2 we investigate the multi-spectral images and their ability to provide an accurate binary image. Chapter 3 deals with the assessment of the different binarization methods and their combination. In Chapter 4, we apply a character spotting technique and show how it can be used for further research of the Dead Sea Scrolls manuscripts.

Chapter 2

Multispectral Image Binarization

2.1 Background

As part of the recent preservation efforts, all the fragments of the Dead Sea Scrolls are being photographed with high resolution multi-spectral cameras. It has long been known that infrared imaging dramatically improve legibility of scrolls that are impossible to read with the naked eye [1]. In this chapter we investigate whether the multi-spectral images in different wavelengths may be utilized to achieve a more accurate binary image, one in which the letters are well identified and the variability in the background has little influence on the result.

For each fragment of the scrolls we have photographs taken at 12 different wavelengths, between 445nm and 924nm (see Figure 2.1). The illumination is identical in all the 12 images and they are perfectly aligned.

When examining the different images, it is clear that the higher the wavelength, the higher the image contrast. This observation was verified by Faigenbaum et al [8], who showed that the image taken at 924nm is the image with the highest contrast among the available images. Therefore, when choosing a single image to use in order to achieve a binary output, this would be the natural choice. However, we assume that the different wavelength images together contain more information than any one alone. The images were combined as part of the binarization process of the scrolls. The binarization is performed using an SVM classifier, where the features of each pixel are its grayscale values in the images of the different wavelength. The following sections describe in details the preprocessing steps, the binarization method, and the results obtained in several experiments.

2.2 Preprocessing Steps

All the images of the scrolls contain the scroll fragment located in the center, as well as a color ruler and an identification tag in the margins. The fragment is fixed by tape, which is also used in some cases to hold several fragment pieces assembled together. These features can be seen in the images of Figure 2.1.

Prior to the binarization step, all these objects were removed and the parchment area was identified by means of the following process:

1. The image with the lowest wavelength (445nm) was subtracted from the one with highest wavelength (924nm). Since the artificial objects appear similar in all wavelengths, this usually leaves only the parchment pieces in the image.

2. The image is thresholded to segment the objects and the black background, and then morphological operations of filling and opening are applied to the objects, to achieve smooth and accurate shapes.

3. The connected components, namely, continuous regions of black pixels, are identified in the resultant binary image. If more than one component is found, the

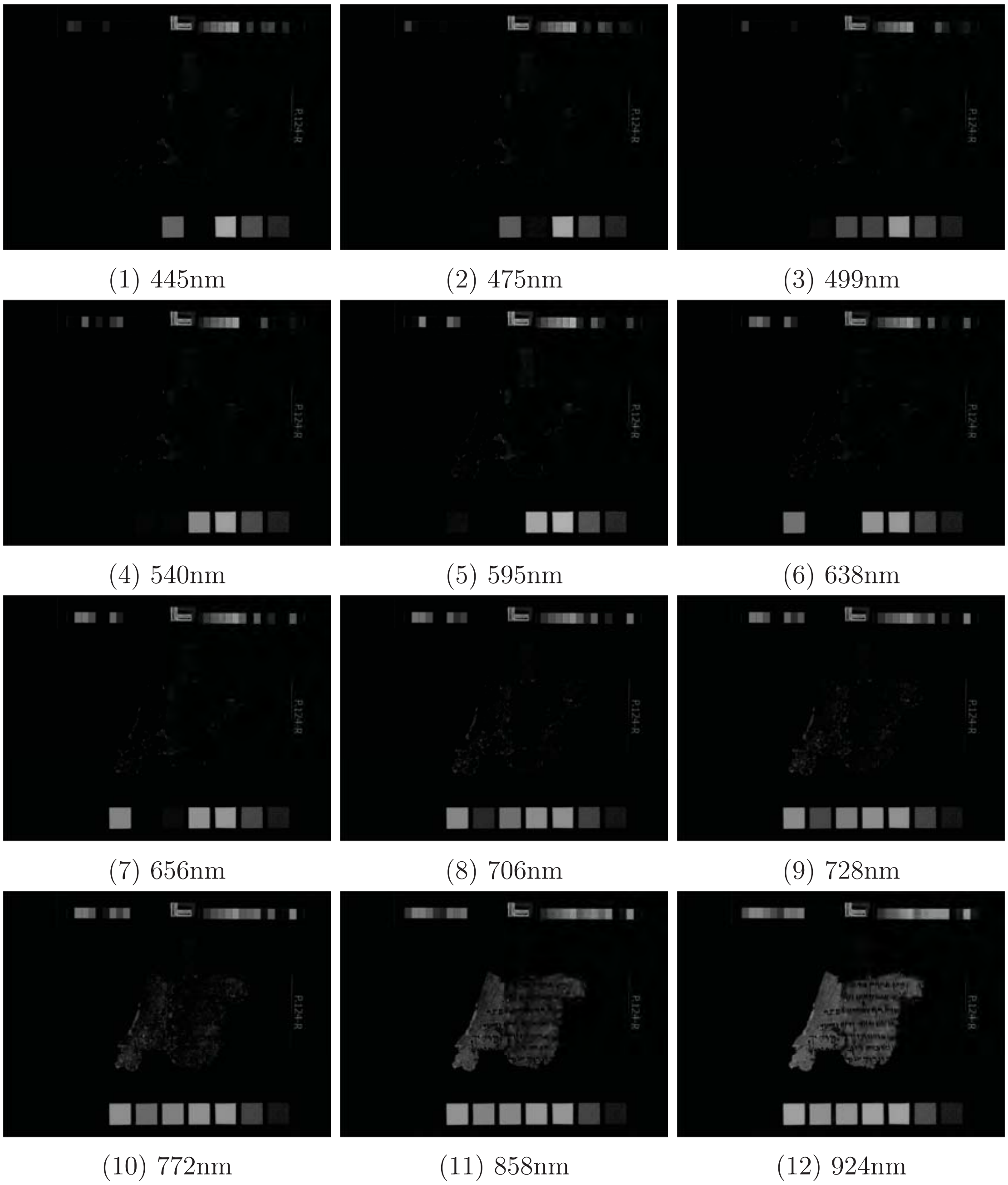

Figure 2.1: Images of a single scroll fragment taken at different wavelengths

parchment is identified as the one that contains the image's central pixel.

All the steps described below were conducted using the masked image achieved by the above steps.

2.3 Binarization Method

The different wavelengths are combined to achieve a binary image by the following method:

1. The baseline for each fragment is the result of Sauvola's method [3] on the single highest wavelength (924nm).

2. Given k different wavelengths ($1 \leq k \leq 12$), we train an SVM classifier using an equal number of foreground and background pixels. The features of each pixel are its gray-scale values in the k different images, scaled to the range $[0, 1]$. The label of each pixel is its value in the baseline binary image.

3. The achieved SVM model is used to classify every pixel in the image as foreground or background, according to its k features. The obtained image is our binary result.

We used LIBSVM [9] code (for Matlab) to create the SVM model and classify.

2.4 Experiments and Results

The method described above was applied to different combinations of wavelengths in order to evaluate the contribution of each of the images to the desired result of an accurate binary image. To evaluate the output obtained from different combinations, manually-made ground-truth binary images are used, and the following measures are calculated:

$S_{\textbf{total}}$ The fraction of pixels that were correctly classified as foreground or background.

$S_{\textbf{fg}}$ The success rate on the foreground area, namely, the fraction of the foreground that was correctly classified.

$S_{\textbf{bg}}$ The success rate on the background area, namely, the fraction of the background that was correctly classified.

To analyze the contribution of different wavelengths, we performed three different experiments. The data set included 18 fragments, each containing images of 12 different wavelengths and a ground-truth binary image. First, each wavelength was used in the above scheme as a single reference. Table 2.1 shows the average scores obtained for each of the wavelengths separately. The results show, as expected, that the high wavelengths produce better results than the lower ones. Additionally, the scores show that while the foreground is well detected in all of the images, the challenging task is the correct identification of the background. In the lowest wavelengths, which are very dark, almost all of the pixels are classified as black, as reflected by the very high foreground success and low

	S_{total}	S_{fg}	S_{bg}
445nm	0.145	0.965	0.091
475nm	0.172	0.959	0.119
499nm	0.201	0.959	0.151
540nm	0.323	0.949	0.283
595nm	0.510	0.935	0.483
638nm	0.644	0.940	0.627
656nm	0.753	0.933	0.744
706nm	0.902	0.937	0.901
728nm	0.933	0.939	0.933
772nm	0.955	0.943	0.956
858nm	0.965	0.950	0.966
924nm	0.964	0.953	0.965

Table 2.1: Average binarization scores of single wavelengths.

background success. As the wavelength increases, the foreground detection significantly improves.

In the second experiment, the effect of incrementally adding and removing each wavelength is tested. First, the model is trained with groups of increasing size, starting with the lower wavelength, and adding a single wavelength at a time up to the whole group of 12 images. The results obtained in this experiment are shown in Figure 2.2a. The plot shows that adding each wavelength increased the success of background identification, and the most significant improvement occurred up to the 8th wavelength. The highest score in this experiment was the score for all wavelengths, with average total success of 0.97. Second, the effect of removing each wavelength is tested by starting with all of the wavelengths, and then removing the lowest one in each step. The results are shown in

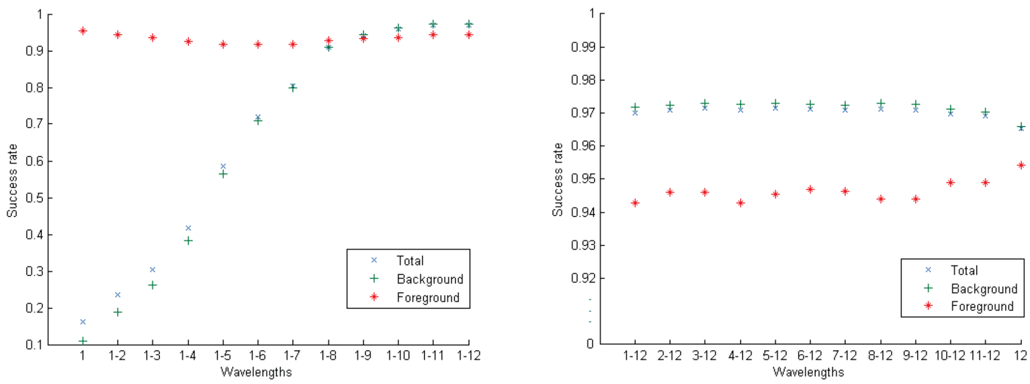

(a) (b)

Figure 2.2: Binarization scores of different groups of wavelengths. The wavelengths are numbered from 1 to 12, in increasing order. In (a), each wavelength is added incrementally, starting with the lowest wavelength. In (b), in each step the lowest wavelength is removed, starting with the group of all 12 wavelengths.

Figure 2.2b. While all of the groups obtained high scores, the plot shows that removing a few of the lowest wavelengths increased the success rate, especially due to better foreground identification. The highest average success of 0.9714 was obtained both by the groups of the highest 10 and of the highest 8 wavelengths.

The results above show that combining multiple wavelengths yields better accuracy of the binary image. However, it is questionable whether the whole group of 12 wavelengths is necessary to obtain this result, since figure 2.2a shows that the improvement is less significant when adding the highest three wavelengths, and figure 2.2b shows that not all of the lower wavelengths are required.

Since testing all the possible groups of wavelengths is not feasible, the final experiment was to perform feature selection for the SVM model to find which wavelengths best predict the ground truth binary image. This was done using a sequential feature selection, performed on a sample of pixels of each fragment in the data set of 18 fragments. The 18 groups of selected wavelengths contained between 1 to 7 wavelengths, with an average of 3.3 wavelengths. Figure 2.3 shows the number of times each wavelength was selected. The most common wavelengths are the two highest wavelengths and the lowest one, and all groups contained at least one of the three highest wavelengths. These result confirm the assumption that using all wavelengths is redundant and that the higher wavelengths are the major contributors to the result, but once one or two of the highest wavelengths were chosen, we may get more from adding a lower one than from adding another high one. Hence, an optimal set of wavelength for image binarization of the scrolls should include wavelengths 1,11 and 12. Such a set will provide both accurate and informative result and an efficient solution.

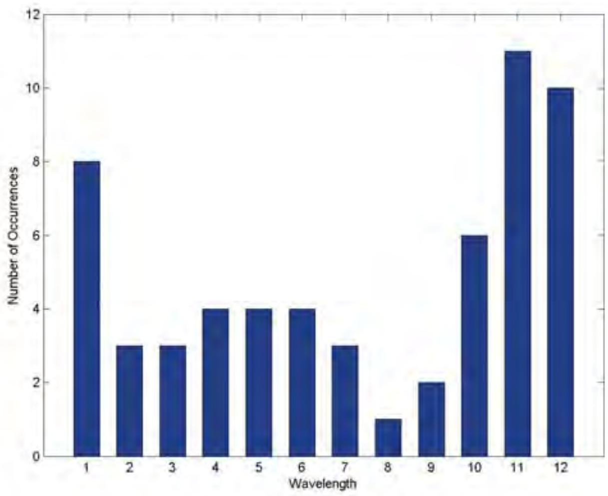

Figure 2.3: Feature selection results for the 12 different wavelengths. The plot shows the number of times each wavelength was selected in the set of experiments.

Chapter 3

Combining Binarization Methods

3.1 Background

Many binarization methods have been suggested to approach the typical problems of historical or damaged documents. In such documents, global methods like Otsu's thresholding [10], usually perform poorly, since tears, stains, and ink fading lead to high variation within one fragment. A global threshold fails to capture all the details, and the outcome contains many black regions that do not represent the document's foreground. The results of local methods like Sauvola's may suffer from the opposite problem: since they only consider the local neighborhood of each pixel, the variation within the letters caused by a damaged parchment or by ink fading leads to under-recognition of letters.

The scroll images are of varying quality: some fragments are highly damaged, while others are well-conserved. The fragments have gone through different kinds of deterioration: tears, stains, and ink fading are very common. As a result, the different available methods produce varying results on the scroll images, as each algorithm is designed to solve a particular problem.

In this section, we consider the results of several state-of-the-art binarization methods on the images of the scrolls, and we suggest a few methods of combining their results. Two approaches are suggested: First, combining the different binarizations by optimizing the result of the next step: the identification of the letters in the image. This step is common to many document image-processing applications that may follow, such as OCR and palaeographic classification. The second approach obtains continuous value for each pixel , representing how confident each method is in its decision, and uses this value to build a more accurate classifier.

3.2 Binarization Methods

This section describes the different binarization methods used in this chapter. The input for all of the methods (except for the multi-spectral method) was the single image of the highest wavelength. The binarization is done only on the parchment area of the image, which was extracted by the pre-processing steps described in Section 2.2.

Otsu

Otsu [10] thresholding computes a single threshold which separates between the two classes, the background and the foreground. This is done by searching for the threshold that maximizes the relation between the within-class variance and the between-class variance of the two classes.

Sauvola

Sauvola algorithm [3] defines a different threshold for each pixel. A sample of pixels in the image is defined as the *base pixels*, for which the threshold is calculated directly, and the threshold for the *non-base pixels* is interpolated from the nearest base pixels. The threshold for a base pixel (x, y) is calculated as follows:

$$T(x, y) = m(x, y)\left[1 + k\left(\frac{s(x, y)}{R} - 1\right)\right]$$

where $m(x, y)$ is the mean of gray level among the pixel's neighborhood, $s(x, y)$ is the local standard deviation, and R is the standard deviation range (usually set to 128). The parameter k is positive and usually defined to be in the range 0.2–0.5. In a high contrast region, $s(x, y) \approx R$, so $T(x, y) \approx m(x, y)$. When the contrast is low, $T(x, y) < m(x, y)$, that is, the threshold is set to a darker gray level.

Bar-Yosef

Bar-Yosef et al. [6] developed a multi-staged binarization method, addressing the specific problems of Hebrew historical documents. A global threshold is applied to achieve an initial binary image, followed by an evaluation procedure of each connected component in these image. This is done by considering the *seed image* of each letter, comprised of its darker pixels. Characters that are identified as noisy are iteratively refined by re-classifying the pixels in the local neighborhood of the seed image.

Su

Su et al. [5] introduced a binarization technique that makes use of the high-contrast regions in the image. First, the high-contrast pixels are located based on the minimum and maximum of the pixel's neighborhood, and a *contrast image* is built, in which only the high-contrast pixels are black. The high-contrast pixels usually lay around the text stroke boundaries. The image is then segmented using local thresholds that are estimated from the detected high-contrast pixels within a local neighborhood window: each pixel is classified according to the number of high-contrast pixels surrounding it, and according to its intensity relative to that of the high-contrast neighbors.

Faigenbaum

Faigenbaum et al. [11] developed a simple method in order to binarize images of ostraca. Given manually marked regions of background and foreground, the grayscale histogram of each class is calculated. Each pixel is assigned to the class in which its value is most common.

Instead of manually selecting foreground and background regions, we used a sampled set of text and background pixels from Sauvola's result.

Multi-spectral

This is the multi-spectral SVM classifier described in Chapter 2, trained with the four highest wavelengths.

Table 3.1 shows the average scores obtained by the different methods on a set of 24 fragments of the scrolls, for which we prepared ground-truth binary images. On this image set, contrary to the different wavelengths results in Table 2.1, the main difficulty seems to be text identification. The reasons for this are the use of only one wavelength and the fact that this set includes more images, some of them containing very faded letters.

	S_{total}	S_{fg}	S_{bg}
Otsu	0.965	0.882	0.971
Sauvola	0.972	0.778	0.987
Bar-Yosef	0.960	0.920	0.963
Su	0.967	0.810	0.980
Faigenboum	0.951	0.851	0.959
Multispectral	0.964	0.900	0.970

Table 3.1: Average binarization scores of the different binarization methods.

3.3 Keypoint Detection and Clustering

3.3.1 Keypoint Detection

The first step in the identification process is calculating the physical measurements of the text lines of each fragment: the height of the lines and the space between the lines. These parameters are calculated using the same method used on the Genizah documents [12], based on the Hough transform of the image. However, in contrast to the Genizah documents, the scrolls contain very small fragments, many of them with very few letters. On such pieces, this method fails to identify the lines, since it assumes that the fragments contain several relatively straight and uniform lines of text.

Therefore, we used the fact that the scrolls were divided by scholars into plates, and the fragments that are grouped together on a plate are assumed to originate from the same scroll and should have common characteristics. The fragments were divided into two groups: *big* fragments, which contain several lines of text, and *small* fragments, in which text lines cannot be identified (see Figure 3.1). First, the physical measurement of the big fragments were calculated using the above method. Then, for the small fragments, the measurements were defined to be the average of the values measured for all the big fragments in the same plate.

The keypoint detection method uses the fact that, in Hebrew writing, letters are usually separated. First, the connected components (CC) of the binarized images are calculated. To filter out fragmented letter parts and fragments arising from stains and border artifacts, we compare the size of the CC to the height of the lines that was estimated in the previous step. Each keypoint frame is encoded to a single vector using the SIFT descriptor [13], which encodes histograms of gradients. The scale of each detected keypoint is taken as the maximum dimension of the associated CC.

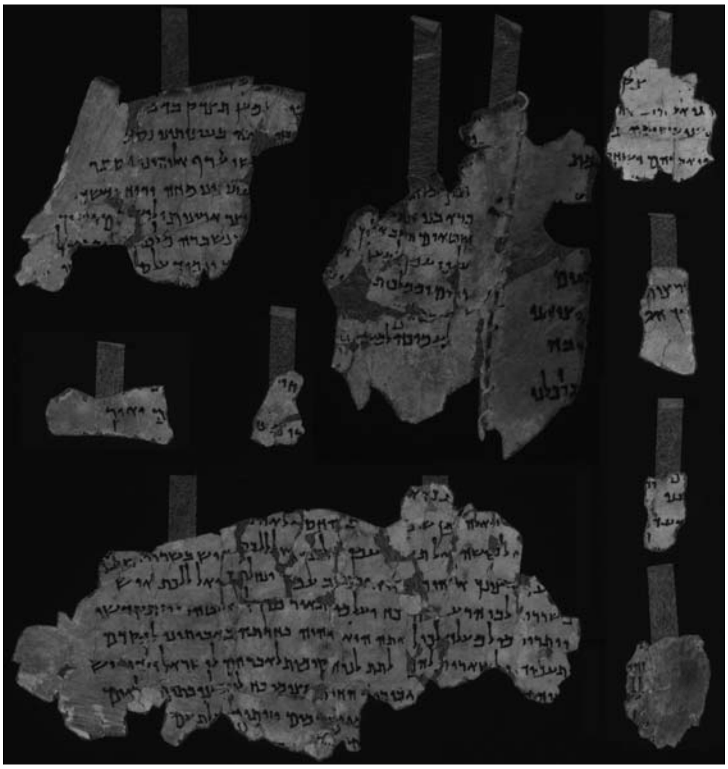

Figure 3.1: An example of a plate (manuscript 4Q393) containing three large fragments and six small ones

3.3.2 Keypoint Clustering

The next step is to cluster the obtained group of descriptors, in order to build a dictionary of all the letters in the fragment. As before, this is an impossible task when we deal with fragments that contain very few letters. Thus, instead of performing the clustering on the fragment level, we perform the clustering on the plate level, obtaining a separate dictionary of the letters for all the fragments on the same plate.

The descriptors of each plate are clustered using the k-means method with Euclidean distance, with $k = 50$. To select the right value of k, we tested the results of different values, between $15 - 105$, and compared the sum of distances between the descriptors and their clusters' centroids. The sum of distances is expected to decrease as k increases, but around the value of 50 the decrease slows down. Therefore, $k = 50$ was chosen as the optimal value.

3.4 Evaluation of Binary Result

Having in mind the goal of the next step – achieving a dictionary of letters by clustering the keypoints - we aim to evaluate the output of the different binarization algorithms by evaluating the clusters extracted from the binary images. A good clustering result has high intra-cluster similarity (letter descriptors within a cluster are similar) and low inter-cluster similarity (descriptors from different clusters are dissimilar). In our case, high intra-cluster similarity indicates that each cluster indeed represents a single letter, and low inter-cluster similarity indicates that the clusters represent different letters. The presence of noise in the binary image, caused by stains, tears, and broken letters, that are mistakenly recognized as keypoints, is expected to lead to poor results in the sense of these two characteristics. We compared three different measures that formalize these two goals:

1. **Davies-Bouldin index** (DB) [14]: Suppose we have N clusters. For each cluster C_i, let S_i be the average of the Euclidean distances between the elements of C_i and their centroid. For each pair of clusters C_i, C_j, let $M_{i,j}$ be the distance between their centroids. For every i, j we define $R_{i,j} = \frac{S_i+S_j}{M_{i,j}}$ as a measure for the quality of the separation between the two clusters, and for each cluster C_i, let $D_i = \max_{j:i\neq j} R_{i,j}$. Then the DB index is defined as:

$$DB = \frac{1}{N}\sum_{i=1}^{N} D_i$$

2. **The ratio** (R) between the intra-cluster and the inter-cluster similarity. Let $\overline{S}$ be the average of the intra-cluster distances, that is, using the notations above, $\bar{S} = \frac{1}{N}\sum_{i=1}^{N} S_i$, and let $\overline{M}$ be the average inter-cluster similarity, $\overline{M} = \frac{1}{N}\sum_{i=1}^{N} M_i$. Then the ratio measure is:

$$R = \frac{\overline{S}}{\overline{M}}$$

3. **The mean distance** (M) between every descriptor and its cluster's centroid. This measures only the intra-cluster similarity of all clusters. Assuming there are n samples, let a_k be the distance between the k'th sample and the centroid of the cluster it is assigned to. Then the score is:

$$M = \frac{1}{n}\sum_{k=1}^{n} a_k$$

3.5 Combination by Clustering Score

3.5.1 Method Outline

In a given fragment, for each pixel we have a decision – black or white - from each expert (binarization method), and each expert has a clustering score as calculated for the particular fragment. The naive way of combining the methods would be to choose the majority vote for each pixel. Using the score of the clustering result, we can use the weighted votes of the experts. Thus, for each pixel x, y we calculate the sum:

$$S_{x,y} = \sum_{i=1}^{k} w_i \cdot d_i$$

where k is the number of experts, d_i is the decision made by the i'th expert (-1 for background, 1 for foreground), and w_i is the clustering score, normalized to the range $[0, 1]$. We assign the value according to the majority, that is:

$$B(x, y) = \begin{cases} 1 & \text{if } S_{x,y} > 0 \\ -1 & \text{otherwise} \end{cases}$$

3.5.2 Experiments and Results

The above method was applied to a set of 230 fragments, from 15 different plates. The three measures described in section 3.4 were tested separately as the weights of the binarization methods. The simple combination by majority vote was also tested. Table 3.2 shows the average clustering scores obtained by the different methods and by the four combinations. Overall, the scores do not seem to improve in the different combinations, compared to the individual methods, and there is little difference between the different combinations. However, in many cases, the keypoint detection in the combined images provides a higher detection rate of the characters in the image, as can be seen in Figure 3.2.

	Ot.	Sa.	BY	Su	Fai.	Mul.	Simple Comb.	DB Comb.	R Comb.	M Comb.
DB	1.64	1.64	1.67	1.65	1.72	1.61	1.72	1.73	1.65	1.72
R	0.51	0.54	0.54	0.52	0.59	0.55	0.65	0.64	0.55	0.65
M	72.2	69.3	73.5	69.9	72.0	69.9	72.7	73.1	72.9	72.8

Table 3.2: Average clustering scores obtained by individual binarization methods and the different combinations.

(a) (b) (c) (d)

Figure 3.2: Keypoints detected in different binary images: Otsu (a), Sauvola (b), Bar-Yosef (c) and the R-combination result (d). While in the individual methods not all the characters are recognized, the combination led to a better recall of the letters.

3.6 Iterative Combination of Binarization Methods

The method described below considers the quality of the clustering with regard to each letter descriptor separately. The best binary result of a single letter is the one that makes it closest to the centroid of the cluster it belongs to. Thus, we try to optimize the achieved result by selecting for each letter individually its best binary representation. This is done in an iterative manner, by the following steps:

1. Separately, for each binary image, the keypoints (candidate letters) are detected. Then, a single set of keypoints is built for each fragment by merging the keypoints from all of the binary images. If the overlap between two keypoints spans more than 90% of their area, only one of them is taken.

2. The obtained keypoints are clustered to achieve the representative letters (the clusters' centroids). This is done on the plate level, for each binary method separately.

3. For each keypoint, the best binarization method is selected locally according to the obtained clusters. The best method is the one that makes the keypoint closest to its centroid.

4. The image keypoints of the new combined image are detected.

5. We go back to 2.

After applying the first iteration, the achieved results seem to be cleaner of noise caused by tears and stains, since detected keypoints in these areas belong to less cohesive clusters. However, parts of the characters also disappear in the binary output, probably for the same reason. This leads to even lower success in the second iteration, which is based on keypoint detection performed on the output of the first iteration. In the future, we suggest trying a different measure for the success of a binarization method for each keypoint, perhaps using the results of the character spotting method described in Chapter 4.

3.7 Confidence Based Combination

3.7.1 Method outline

This method uses the output of different binarization methods to classify each pixel separately, considering how confident each expert is in its decision. For each pixel, instead of a binary value (-1 or 1), we extract a continuous value, between -1 and 1,where -1 means it is a background pixel and 1 means it is foreground. This value is the *confidence* value, and the closer it is to one of the ends, the more confident the method is with the classification of the pixel. After achieving a confidence value for each method, a two-step SVM model is built in the following way:

1. An auxiliary SVM model is trained for each method, where each pixel in the sampled set is represented by the method's confidence value, and the output is the method's decision for this pixel.

2. For each method, each pixel is classified using the trained SVM, and its confidence level is extracted, namely, the signed distance of the pixel from the supporting vector (negative for pixels classified as -1, positive otherwise).
3. An SVM classifier is trained, where the features of each pixel are the different confidence measures obtained from the previous step. The labels are taken from a binary outcome of a method that is not included in the combination.
4. The combined model is applied to each pixel, to achieve the binary image.

3.7.2 Confidence measure

Below is the description of the confidence-measure calculation for each of the binarization methods that were included in the combination. The input grayscale image is denoted by I.

Otsu

Otsu's method provides a global threshold T, and classifies the pixels above T as white, and the pixels below T as black. The confidence measure of each pixels is the difference between the threshold and the pixel's gray level:

$$C(x, y) = \frac{T - I(x, y)}{255}$$

This value will be positive for foreground pixels, and negative for background pixels. It is normalized by 255, which is the highest possible difference.

Sauvola

Sauvola's algorithm calculates a different threshold $T_{x,y}$ for each pixel (x, y). Thus, the confidence measure of each pixel is the distance between the pixel and its threshold:

$$C(x, y) = \frac{T_{x,y} - I(x, y)}{255}$$

Su

Su's method first detect the *high-contrast* pixels in the image and then uses two parameters to make the decision on each pixel (x, y): $N_{x,y}$, the number of high-contrast pixels within the pixels' neighborhood, and the difference between the pixel's gray value, $I(x, y)$ and the average gray value of the high-contrast pixels in the neighborhood. The classification rule is:

$$B(x, y) = \begin{cases} 1 & \text{if } N_{x,y} \geq N_{min} \text{ and } I(x, y) \leq \frac{E_{mean}+E_{std}}{2} \\ 0 & \text{otherwise} \end{cases}$$

where N_{min} and the window size, w, are defined according to the average stroke width in the image, and E_{mean} and E_{std} are the mean and standard deviation of the contrast pixels within the local window. The confidence is also based on these two components, and it measures the distance of each pixels from the two thresholds, giving equal weight to both scores:

$$C(x,y) = 0.5\frac{N_{x,y} - N_{min}}{w^2} + 0.5\frac{(E_{mean} + E_{std})/2 - I(x,y)}{255}$$

Faigenboum

This method calculate the histogram of gray levels of the n points sampled from the reference image for both classes (foreground and background) and assigns each pixel to the class where it was most frequent. The confidence for a given gray level is the difference between its frequency in the two classes. The larger the difference, the more confidence the classification of this method:

$$C(x,y) = \frac{H_{fg}(I(x,y)) - H_{bg}(I(x,y))}{n}$$

Where H_{fg}, and H_{bg} are the foreground and background histograms, respectively.

Multi-spectral

The classification is performed using an SVM classifier, and the confidence value is the decision value returned by the LIBSVM method. The values corresponds to the distance from the separating vectors, where the sign of the value corresponds to the classification of the pixel (negative for -1 ,positive for 1).

3.7.3 Experiments and Results

We tested different combinations of the above 5 methods, using Bar-Yosef's method as the baseline outcome, since it was not included in the combination, and achieved relatively high scores on the tested fragments (see Table 3.1). Table 3.3 shows the score obtained by the best 3 combinations, on the set of 24 images with ground-truth references. The results show much improvement in the foreground detection with respect to the original methods, while the foreground detection success is still high. Figure 3.3 shows the results of a particular fragment in which ink fading led to very low foreground detection in the different methods. However, the combination of methods managed to reconstruct the text using the information of the methods' confidence and the relatively good result of Bar-Yosef as baseline.

	S_{total}	S_{fg}	S_{bg}
Otsu+Sau.+Su+Multi.+Fai.	0.947	0.962	0.946
Otsu+Sau.+Su+Multi.	0.947	0.963	0.946
Otsu+Sau.+Su.	0.947	0.962	0.946

Table 3.3: Average binarization scores of the confidence based method, using different combinations of methods.

(a) Original image (b) Bar-Yosef (c) Otsu (d) Sauvola

(e) Su (f) Faigenboum (g) Multispectral (h) Combination

Figure 3.3: Results of the different binarization methods: (a) is the input grayscale fragment; (b) is Bar-Yosef's result, which was used as baseline; (c)–(g) are the output of the different methods, and (h) is the result of the combination of all five methods.

Chapter 4

Character Spotting

4.1 Background

Searching for a letter or a word in historical documents is a challenging task. Traditional optical character recognition (OCR) methods do not perform well on such documents, as degradation and different kinds of damages lead to broken and smeared characters, holes, and other artifacts. As an alternative to OCR, a word spotting technique was proposed [15]. The main idea of word spotting is that the search is performed on the images without converting them to textual representation. The goal is to find all the sub-images in the document image that are similar to the given query image.

Character searching in the Dead Sea Scrolls is challenging due to some unique features of this data set. First, the Scrolls are written in a Hebrew alphabet, which is characterized by a high similarity among letters. Second, since many fragments are damaged and degenerated, characters frequently appear broken or partial. Finally, the scrolls were written by many different authors and contain a variety of handwritings, as well as special scribal markings, some of which are of unknown meaning.

Instead of searching the whole fragment, we use the detected keypoints obtained by the method described in Chapter 3.3.1 as candidate characters, and we try to match each one of them the query character. We use a Dynamic Time Warping algorithm, which was proved effective in similar word spotting tasks [16]. The main advantage of this algorithm is the ability to measure the similarity between images of varying size. This is important since the scrolls were written by hand, so the size of the characters is not uniform even within the same fragment.

In [17], different column features were suggested to identify a query word. Rabaev et al. [18] presented special features that deal with the special characteristics of the Hebrew script. We tested the usability of a set of similar features on the scrolls, using them both as column and row features. We also tested the matching of partial letters, aiming to achieve better recall of relevant characters. We suggest a few applications of this method that in the future may facilitate the recognition of joins and the identification of the period in which a fragment was written. Additionally, the character spotting can be extended to a word spotting technique, and it can be used as part of an OCR mechanism.

4.2 Feature Extraction

The algorithm measures the similarity between a set of features extracted for the query and the candidate letter. The features are extracted for each column of pixels in the image. The following features were tested:

1. Projection profile (PP): the number of black pixels in the column.
2. Upper/Lower character profile (UP/LP): the location of the upper/lower black pixel
3. Transition profile (TP): The number of transitions between background and foreground pixels in the column.
4. The distance between the upper and lower boundaries of the column ($DULP$).

As opposed to word spotting, when matching a single character, the row profile may be as informative as the column profile. Thus, for each candidate, the above features were extracted twice, once for the columns and once for the rows (applied to the transposed image). Figure 4.1 demonstrate the different column features.

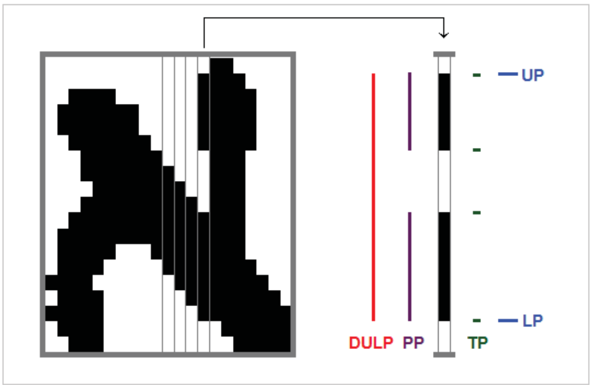

Figure 4.1: The column features extracted for each letter

4.3 Matching algorithm

Given a query character and a candidate character, the feature vectors of both of them are compared using a Dynamic Time Warping algorithm (DTW). The DTW method performs a non-linear sequence alignment, which is suitable for handwritten text, in which we expect to find variation in size even within instances of the same letter.

Each character is represented by a set of m d-dimensional vectors, where m is the window width and d is the number of features. Given two character windows, A and B, the DTW matching algorithm simultaneously aligns the two sets of feature vectors, F_A and F_B, by finding a path that matches them, using the recurrence equation:

$$DTW(i,j) = dist(F_A(i), F_B(j)) + min \left\{ \begin{array}{l} DTW(i-1,j) \\ DTW(i,j-1) \\ DTW(i-1,j-1) \end{array} \right\}$$

where $dist(\cdot,\cdot)$ is the squared Euclidean distance between the two d-dimensional vectors, representing the i'th column of A and the j'th column of B. The matching error for matching the two images, A and B, is defined as:

$$err(A,B) = \frac{1}{l} DTW(F_A, F_B)$$

where l is the length of the warping path recovered by the algorithm.

4.4 Experiments and Results

4.4.1 Feature selection

The performance of the different features was tested on two relatively big fragments, in different preservation conditions: one is well preserved, while the other contains many tears and holes. The binary image we used is the result of the R-combination described in Section 3.5, since the keypoint detection in this result achieved high recall of the characters in the image. The two images together contain 524 candidate characters, each was assigned the correct classification, i.e. the Hebrew letter it represents (numbered starting from 1), or 0 for no letter. Four query characters were selected for each fragment, and their images were cut from the fragments' binary images. The selected letters are relatively frequent in the fragments. Figure 4.2 shows the two images and the query letters used for each of them.

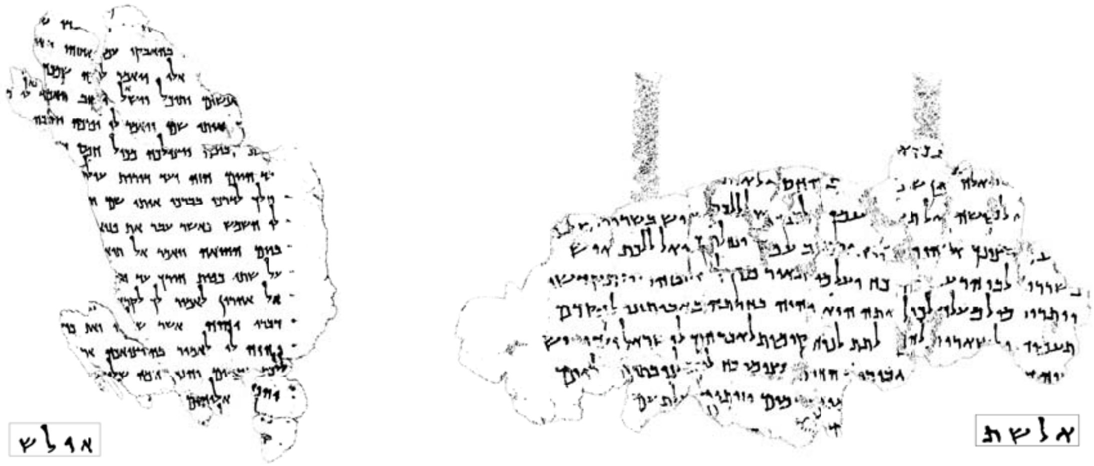

(a) (b)

Figure 4.2: The fragments used for the features testing, and the query letters taken from each of them

First, we compared the performance of using column feature and row features. We ran three experiments, with the five features described above: (1) using the score obtained from the column features, (2) using the score obtained from the row features, and (3) using the the average of the two scores. Figure 4.3 shows the ROC curves obtained using these three scores. Overall, the row features' performance was much better than both the column features and the average of scores. This makes sense, as many Hebrew characters have common upper or lower profiles, but the horizontal profiles are more variable.

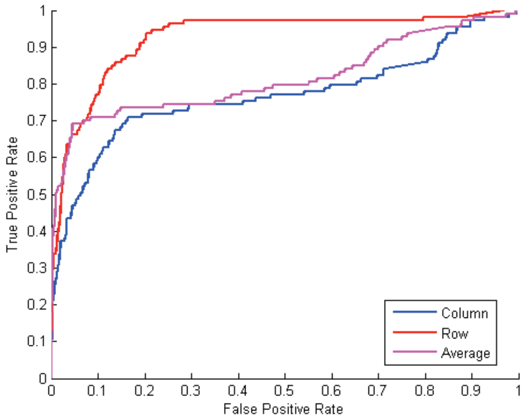

Figure 4.3: ROC curve for matching scores using column features, row features, and both

Next, we tested each of the features separately as row features. Figure 4.4a shows the ROC curve of each of the single features. The best features are *UP*, *DULP* and *PP*. This is consistent with the results reported in [18], claiming that the best features are *DULP* and *PP*. We added the *UP* feature, which captures the left contour of the letter (when used as a row feature) and seems to perform very well.

Figure 4.4b shows the performance of groups of row features. We started with the *DULP* and *PP* features, and tested the effect of adding more features. As expected the addition of *UP* gives the greatest improvement, and no significant improvement is achieved by adding the other features to these three.

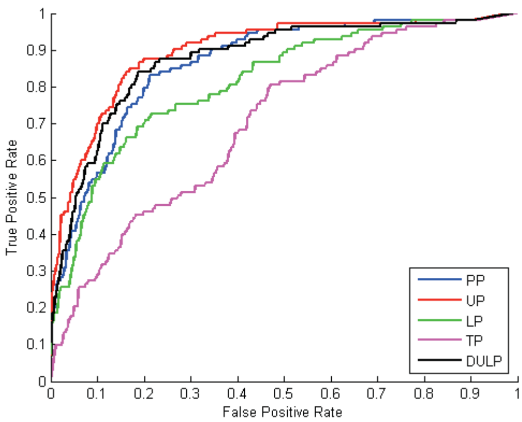

(a)

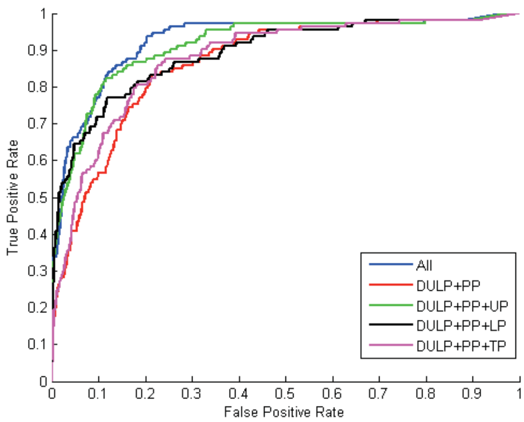

(b)

Figure 4.4: ROC curves for matching with the different features (a) separately and (b) with different groups of features

4.4.2 Matching Partial Characters

The Dead Sea Scrolls are characterized by many tears, small torn pieces and fragments that have deteriorated along the margins, leading to the appearance of broken letters. Since the keypoint detection method assumes that the letters are connected, broken letters will probably be split into more than one keypoint, and the method above will fail to match them to the correct reference letter. To address this, we tested the concept of partial character matching: when a match is not found between the candidate keypoint and the reference letter, we attempt to perform a match between the keypoint and parts of the reference letter. Although this approach was able to identify more correct keypoints, it also caused a decrease in precision, since parts of letters have fewer unique characteristics, and they achieved a high matching score with many irrelevant keypoints. This is demonstrated in Figure 4.5, which shows the results of matching the letter lamed and two partial images of it. While the partial matches managed to identify some instances of the letter that were not discovered by the whole letter, they also matched many wrong letters and their precision is much lower than that of the whole letter.

Figure 4.5: Character and partial character matching results of the Hebrew letter lamed. The legend shows the query letters used. The red frames are the keypoints matched to the whole letter, and the blue and magenta frames are the matches of the upper and lower parts, respectively.

4.5 Applications

4.5.1 Script Identification

We examined the ability of the character spotting method to distinguish between different Hebrew scripts. The scrolls were written in many different Hebrew scripts, and the identification of the fragment's script may help join scroll fragments together and provide some knowledge about the fragment's origin. We used a table of Hebrew scripts of the scrolls, taken from [19] (see Figure 4.6). The table contains 16 different scripts, named according to the manuscript they appear in. We matched each letter separately to each of the candidate letters in a set of 200 fragments, taken from 10 different plates. We found that the different scripts yield different matching results, that is, for any particular Hebrew letter that appears in the fragments, we had 11–16 different query characters of

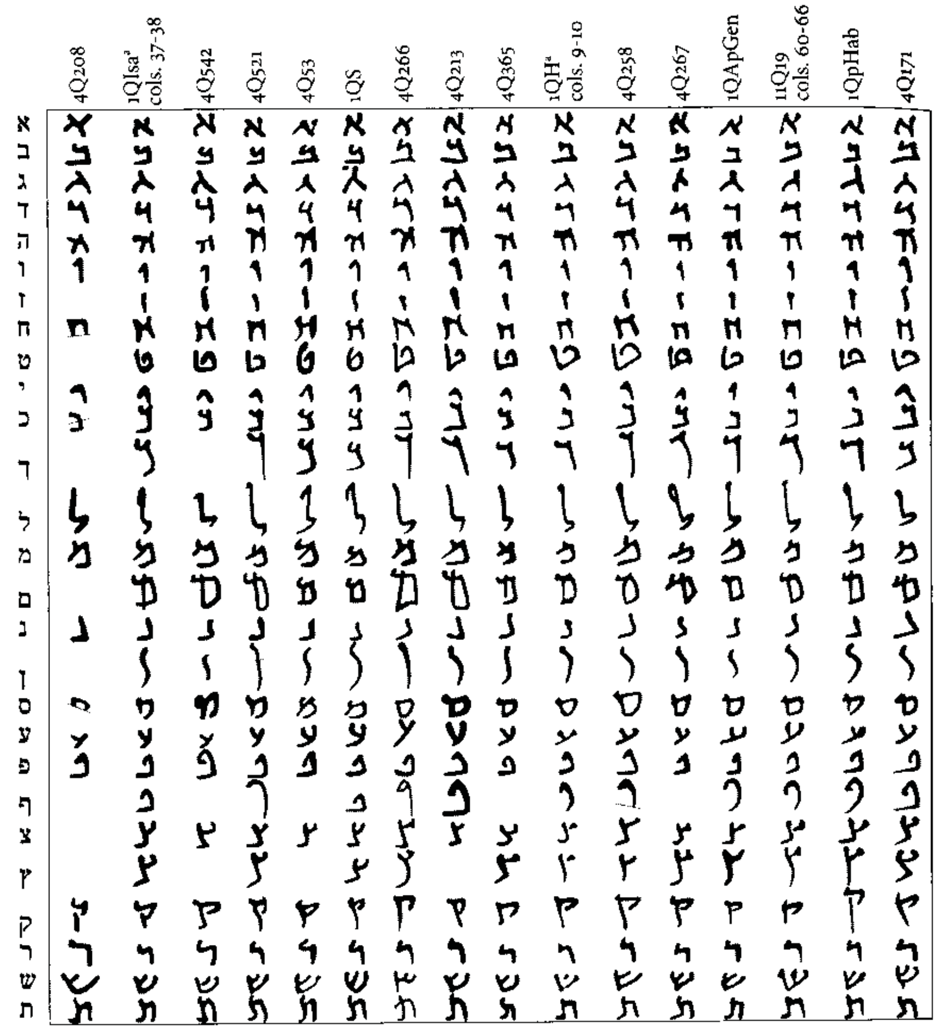

Figure 4.6: The different Hebrew scripts of the Dead Sea Scrolls that were used for matching

the same letter, but only few found it as a match, hinting that the method is sensitive enough to capture the characteristics of different scripts.

We counted for every plate the number of matches from each script found in it. Figure 4.7 shows the results for plate 807, which contains images of manuscript 4Q365, one of the availabe scripts in the table. This was indeed the script with the highest number of matches in the fragments of this plate.

4.5.2 Matching Small Fragments

The next experiment consisted of cutting letters from very small fragments containing one or two letters, and searching for matches within the whole set. For example, we searched for the two letters in the fragment that appears in Figure 4.8a, taken from plate 397 (manuscript 4Q1). The fragment contain the Hebrew letters aleph and tav. Due to damage that occurred to the parchment, the binary images of the letters contained holes, which were filled in the query images, to achieve the accurate shape of the character.

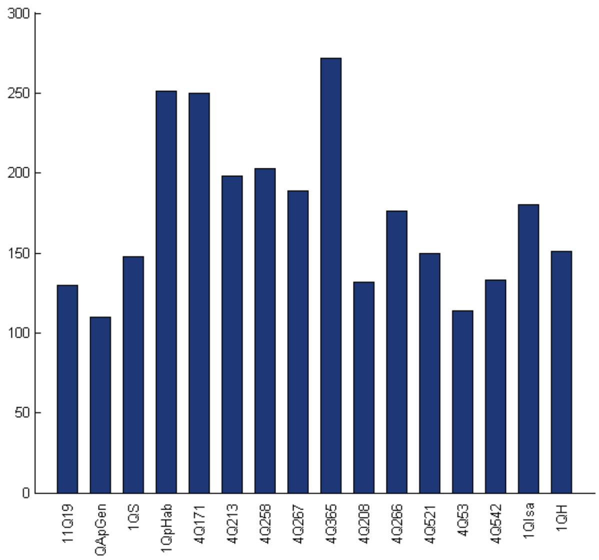

Figure 4.7: The number of matches of the different script in the fragments of plate 807.

We searched for matching characters in the set of 200 fragments, taken from 10 different plates. Figure 4.8b shows the number of matches found for each of the two letters, in each of the tested plates. The majority of the matchings of the letter aleph belong to plate 397, while the results of the letter tav don't show a clear preference to one of the plates. These results imply that in some cases matching the characters may be helpful in learning about the origin of small fragments.

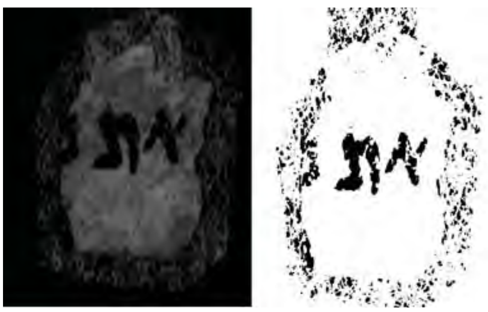

(a) The fragment from plate 397 from which the letters were taken (original and binary).

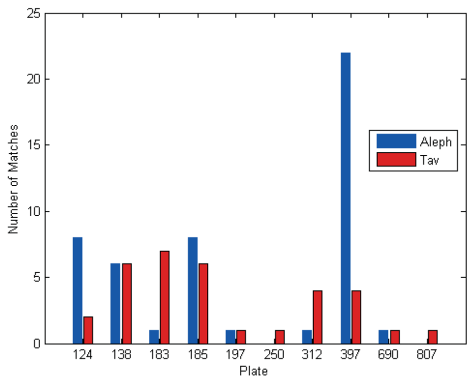

(b) The number of matches of the two letters in the different plates.

4.5.3 Character Recognition

After performing matching with each of the reference scripts, we tried to use the results to identify the characters. Each keypoint that was matched to one or more query letters was assigned a letter in the following way: The most common letter among the matching letters was chosen, and if there was a tie, the one with the best average matching score wins. We tested this method on the two fragments in Figure 4.2. The success rate was 63% for the fragment of 4.2a, and 53% for the fragment in 4.2b. This initial result may be improved in the future by considering the relevant scripts and by performing more processing of the results, such as measuring the similarity between candidates that are assigned to the same letter.

Chapter 5

Conclusions and Further Research

The Dead Sea Scrolls are considered by many to be the greatest archaeological discovery of the twentieth century. They continue to excite scholars as well as lay people due to their great antiquity and the light they shed on the origins of Judaism and Christianity. The use of modern computerized tools may contribute to the resolution of remaining open questions related to the scrolls research, such as who wrote the scrolls, or, rather, to which community or communities did the writers belong.

This work has taken a few first steps towards computer-aided research of the Dead Sea Scrolls. We started with the fundamental step of image binarization, and developed two ways of achieving high-quality binary images of the scrolls. The first is based on the multi-spectral images taken at different wavelengths. We showed that a combination of several different wavelengths provides a more accurate binary image than any single one of them. This confirms the assumption that the infrared images contain valuable information and may improve image legibility.

The second binarization method utilizes the advantages of several state-of-the-art binarization methods that were developed to solve common problems in binarization of document images. We showed that using the information of how confident each method is in its decision regarding each pixel allowed the building of a more accurate classifier. This method was able to reconstruct the foreground of fragments even in cases where the ink has faded.

Finally, we applied a character spotting technique to search for and to identify the letters in the scroll fragments. This method makes use of features that can differentiate between Hebrew letters with high accuracy. We showed that this method is able to distinguish between different Hebrew scripts and thus, in the future it may be utilized to determine which fragments are written by the same scribe, and to piece together fragmented scrolls. Additionally, the character spotting method can be used to build a character recognition system for the Dead Sea scrolls fragments, as well as a platform for word searching in the text.

Bibliography

[1] Gregory Bearman. Imaging the dead sea scrolls for conservation purposes. *SPIE Newsroom. 29th December*, 2008.

[2] The Leon Levy Dead Sea Scrolls digital library website. `http://www.deadseascrolls.org.il/home`.

[3] Jaakko Sauvola and Matti Pietikäinen. Adaptive document image binarization. *Pattern Recognition*, 33(2):225–236, 2000.

[4] Yibing Yang and Hong Yan. An adaptive logical method for binarization of degraded document images. *Pattern Recognition*, 33(5):787–807, 2000.

[5] Bolan Su, Shijian Lu, and Chew Lim Tan. Binarization of historical document images using the local maximum and minimum. In *Proceedings of the 9th IAPR International Workshop on Document Analysis Systems*, pages 159–166. ACM, 2010.

[6] Itay Bar-Yosef, Isaac Beckman, Klara Kedem, and Itshak Dinstein. Binarization, character extraction, and writer identification of historical hebrew calligraphy documents. *International Journal of Document Analysis and Recognition (IJDAR)*, 9(2-4):89–99, 2007.

[7] Lior Wolf, Nachum Dershowitz, Liza Potikha, Tanya German, Roni Shweka, and Yaacov Choueka. Automatic paleographic exploration of genizah manuscripts. *Codicology and Palaeography in the Digital Age II*, 2:6, 2011.

[8] Shaus A. Sober B. Turkel E. Piasetzky E Faigenbaum, S. Potential contrast evaluation - the best of all possible images.

[9] Chih-Chung Chang and Chih-Jen Lin. LIBSVM: A library for support vector machines. *ACM Transactions on Intelligent Systems and Technology*, 2:27:1–27:27, 2011. Software available at `http://www.csie.ntu.edu.tw/~cjlin/libsvm`.

[10] Nobuyuki Otsu. A threshold selection method from gray-level histograms. *Automatica*, 11(285-296):23–27, 1975.

[11] Shira Faigenbaum, Barak Sober, Arie Shaus, Murray Moinester, Eli Piasetzky, Gregory Bearman, Michael Cordonsky, and Israel Finkelstein. Multispectral images of ostraca: acquisition and analysis. *Journal of Archaeological Science*, 2012.

[12] Lior Wolf, Liza Potikha, Nachum Dershowitz, Roni Shweka, and Yaacov Choueka. Computerized paleography: Tools for historical manuscripts. In *Image Processing (ICIP), 2011 18th IEEE International Conference on*, pages 3545–3548. IEEE, 2011.

[13] David G Low. Distinctive image features from scale-invariant keypoints. *International Journal of Computer Vision*, 60(2):91–110, 2004.

[14] David L Davies and Donald W Bouldin. A cluster separation measure. *Pattern Analysis and Machine Intelligence, IEEE Transactions on*, (2):224–227, 1979.

[15] R Manmatha and WB Croft. Word spotting: Indexing handwritten archives. *Intelligent Multimedia Information Retrieval Collection*, pages 43–64, 1997.

[16] Toni M Rath and Raghavan Manmatha. Word image matching using dynamic time warping. In *Computer Vision and Pattern Recognition, 2003. Proceedings. 2003 IEEE Computer Society Conference on*, volume 2, pages II–521. IEEE, 2003.

[17] Toni M Rath and Raghavan Manmatha. Features for word spotting in historical manuscripts. In *Document Analysis and Recognition, 2003. Proceedings. Seventh International Conference on*, pages 218–222. IEEE, 2003.

[18] Irina Rabaev, Ofer Biller, Jihad El-Sana, Klara Kedem, and Itshak Dinstein. Case study in hebrew character searching. In *Document Analysis and Recognition (ICDAR), 2011 International Conference on*, pages 1080–1084. IEEE, 2011.

[19] Martin G Abegg Jr. The linguistic analysis of the dead sea scrolls: More than (initially) meets the eye. *Rediscovering the Dead Sea Scrolls: An Assessment of Old and New Approaches and Methods*, page 48, 2010.